Exp.-Nr.: A1/01–00
Eingang: 20.12.00
an PAC:

# Mainz Microtron MAMI

**Collaboration A1:** "Virtual Photons"

**Spokesperson:** R. Neuhausen

**Proposal for an Experiment**

**Double Polarization Virtual Compton Scattering in the threshold regime**


**Collaborators:**

N. D'Hose*, E. Burtin, M. Garçon, P. A. M. Guichon, S. Kerhoas-Cavata, J. Marroncle
*(DAPNIA-SPhN CEA-Saclay F91191 Gif-sur-Yvette Cedex, France)*

P. Bartsch, D. Baumann, R. Böhm, M. Ding, M. O. Distler, S. Derber, D. Elsner, J. Friedrich, S. Hedicke, P. Jennewein, F. Klein, K. W. Krygier, H. Merkel*, K. Merle, P. Merle, U. Müller, R. Neuhausen, M. Seimetz, H. Schmieden, A. Süle, G. Tamas, M. Vanderhaeghen, Th. Walcher, M. Weis
*(Institut für Kernphysik, Johannes Gutenberg-Universität Mainz)*

J. M. Friedrich
*(Physik-Department, Technische Universität München, D-85748 Garching)*

R. Van de Vyver, L. Van Hoorebeke
*(SSF, University of Gent, Proeftuinstraat 86, B9000 Gent, Belgium)*

B. Pasquini
*(ECT, Villazzano, I38050 Trento, Italy)*

*Contact Person, *e-mail:* ndhose@cea.fr, Merkel@kph.uni-mainz.de

**Abstract**

The Virtual Compton Scattering experiment in the threshold regime performed at MAMI at $Q^2 = 0.33$ GeV$^2$ seems to indicate a large contribution of the spin-dependent polarizabilities which is predicted by the chiral models. This study can be pursued with a double polarization experiment in order to disentangle the scalar and spin-dependent polarizabilities. The study requires a very good expertise of the complete experimental set-up and an excellent accuracy accumulated during a long period. So in order to define the best strategy and to control the different problems inherent to this polarization asymmetry measurement, we would like to do a first measurement during 300 hours.

# 1 Physics Motivations

A fundamental problem of subatomic physics is to understand the internal structure of the nucleon. Though the small distance structure is very well described by point-like quarks and gluons, its structure at larger distance is not so well understood. There exists many models ranging from constituent quark models to chiral models with pion cloud. Until now, the electromagnetic structure of the nucleon has been investigated with elastic electron scattering, deep-inelastic scattering, and real Compton scattering. Virtual Compton scattering (VCS) is also a fundamental exclusive reaction which may shed a new light on the nucleon structure. VCS off the proton refers to the reaction $\gamma^* p \to \gamma p$ where $\gamma^*$ and $\gamma$ stand for an incoming virtual photon of four-momentum $q$ ($Q^2 = -q^2$) and an outgoing real photon of four-momentum $q'$, respectively. This reaction is accessed experimentally through photon electroproduction $ep \to ep\gamma$. The corresponding Feynman diagram is indicated in Fig. 1. VCS below pion production threshold, can be understood as electron

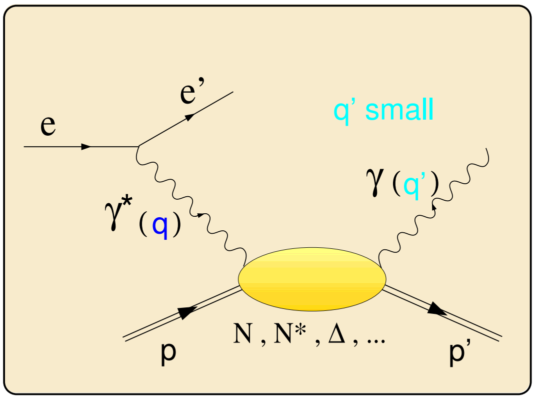


Figure 1: *The investigated VCS diagram*

scattering off a proton which is placed in the quasi-constant electromagnetic field of the outgoing, low-energetic photon. Note that the momentum of the virtual photon q defines the scale for the observation, while the small momentum of the outgoing real photon q′ defines the scale of the electromagnetic perturbation. Analogously to the form factors for elastic scattering, which describe the charge and magnetization distributions, VCS gives access to the deformation of these distributions under the influence of the electromagnetic field. The corresponding observables are 6 generalized polarizabilities (GPs($Q^2$)) [1, 2, 3], of which two are an extension of the well known electric ($\alpha_E$) and magnetic ($\beta_M$) polarizabilities measured in real Compton scattering [4] ($Q^2$=0). At present the GPs have been calculated in the framework of various theoretical models, yielding quite different results both with regard to their absolute value and their $Q^2$ dependence [5, 6, 7, 8, 9]. The GPs are sensitive to the respective role of quark and pion degrees of freedom and as such they are very valuable new observables to confront theory with experiment. An unpolarized VCS experiment allows us to get only two linear combinations of GPs. To separate the GPS we have to resort to a double polarization VCS experiment.

# 2 Unpolarized VCS experiments

## 2.1 Theoretical Framework

The general theoretical framework for VCS has been extensively described by Guichon *et al.* [1, 3] and Drechsel *et al.* [2] and only the relevant points will be discussed here. In the reaction $ep \to ep\gamma$, the final photon can be emitted either by the electrons, refering to the Bethe-Heitler (BH) process, or by the proton, giving access to the VCS process. The BH process dominates and interferes strongly with the VCS process. The amplitude is the sum of the BH, Born and Non-Born amplitudes. The two last-named refer to the proton radiation; the Born amplitude depends only on the static properties of the proton (charge, mass) and elastic form factors, while the Non-Born amplitude contains internal structure information in terms of generalized polarizabilities. In the low energy limit of the final photon, the cross section is independent of the electromagnetic perturbation of the nucleon structure [10], and can be evaluated using only the known BH and Born amplitudes. This can be summarized by the following equation:

$$d^5\sigma^{exp}(\mathrm{q},\mathrm{q}',\epsilon,\theta,\varphi) = d^5\sigma^{BH+Born}(\mathrm{q},\mathrm{q}',\epsilon,\theta,\varphi) + \phi\mathrm{q}'\Psi_0(\mathrm{q},\epsilon,\theta,\varphi) + \phi\mathcal{O}(\mathrm{q}'^2) \qquad (1)$$

where $d^5\sigma$ is a notation for the differential cross section $d^5\sigma/d\mathrm{k}'_{lab}[d\Omega_e]_{lab}[d\Omega_p]_{CM}$, wherein $\mathrm{k}'_{lab}$ is the modulus of the outgoing electron momentum, q and q$'$ are the moduli of the three-momenta of the virtual and real photon (in the photon-proton Centre of Mass) respectively, $\epsilon$ is the virtual photon polarization and $\theta$ and $\varphi$ are the two spherical angles indicating the CM real photon direction on a globe with the virtual photon as a pole. $\theta$ is the CM angle between the real and virtual photons while $\varphi$ represents the angle between the two electron plane and the photon-proton plane. $\phi$ stands for a phase space factor. $\Psi_0(\mathrm{q},\epsilon,\theta,\varphi)$ is the leading term in the expansion in powers of the real photon momentum q$'$. It contains the internal structure information of the proton, parametrized by 6 generalized polarizabilities given for the electric and magnetic dipole radiation of the outgoing real photon.

If we note $L(L')$ the initial (final) photon orbital angular momentum, $\rho(\rho')$ the type of multipole transition (0 for Coulomb, 1 for Magnetic, 2 for Electric) , and $S$ the type of the transition at the nucleon side (non-spin-flip $S = 0$ and spin-flip $S = 1$), the conservation of parity and angular momentum determines 10 GPs presented in table 1. Crossing symmetry and charge conjugation invariance provide 4 relations between the 10 GPs and we are left with 6 independent GPs : 2 scalar ($S = 0$) and 4 spin-dependent ($S = 1$) polarizabilities, functions of q (or equivalently $\tilde{Q}^2 = Q^2|_{\mathrm{q}'=0}$). The choice of 6 GPs is a priori arbitrary, and is realized by the 6 surrounded GPs in the table 1.

In an unpolarized measurement, $\Psi_0(\mathrm{q},\epsilon,\theta,\varphi)$ can be written as:

$$\Psi_0(\mathrm{q},\epsilon,\theta,\varphi) = v_1(\theta,\varphi,\epsilon)(\mathbf{P_{LL}}(\mathrm{q}) - \mathbf{P_{TT}}(\mathrm{q})/\epsilon) + v_2(\theta,\varphi,\epsilon)\mathbf{P_{LT}}(\mathrm{q}) \qquad (2)$$

where $v_1(\theta,\varphi,\epsilon)$, $v_2(\theta,\varphi,\epsilon)$ are known kinematical factors. $\mathbf{P_{LL}}(\mathrm{q})$, $\mathbf{P_{TT}}(\mathrm{q})$, $\mathbf{P_{LT}}(\mathrm{q})$ are structure functions related to the GPs(q) with some kinematical factors $a, b, c_{1,2,3}, d_1$:

$$\begin{aligned} \mathbf{P_{LL}} &= aP^{(01,01)0} \\ \mathbf{P_{TT}} &= c_1P^{(11,11)1} + c_2P^{(01,12)1} \\ \mathbf{P_{LT}} &= bP^{(11,11)0} + c_3(P^{(11,00)1} + d_1P^{(11,02)1}) \end{aligned} \qquad (3)$$

Table 1: *List of the 10 GPs with the corresponding electromagnetic transitions. Their relation with the polarizabilities obtained in real Compton scattering are indicated, as well as the concerned excited states of the nucleon. 6 GPs are independent. Our choice is a priori arbitrary, and is indicated by the 6 emphasized GPs.*

| EM transition | | VCS GPs | $\xrightarrow{Q^2\to 0}$ | RCS polariz. | units | N resonance |
|---|---|---|---|---|---|---|
| $\mathcal{M}^{(C0\to M1)S=1}$ | : | $\boxed{P^{(11,00)1}}$ | $\to$ | $0$ | $fm^2$ | P11 |
| $\mathcal{M}^{(C2\to M1)S=1}$ | : | $\boxed{P^{(11,02)1}}$ | $\to$ | $-\sqrt{\frac{8}{27}}\frac{4\pi}{e^2}(\gamma_2+\gamma_4)$ | $fm^4$ | P33 |
| $\mathcal{M}^{(M1\to M1)S=0}$ | : | $\boxed{P^{(11,11)0}}$ | $\to$ | $-\sqrt{\frac{8}{3}}\frac{4\pi}{e^2}(\beta_M)$ | $fm^3$ | P33,P11 |
| $\mathcal{M}^{(M1\to M1)S=1}$ | : | $\boxed{P^{(11,11)1}}$ | $\to$ | $0$ | $fm^3$ | P33,P11 |
| $\mathcal{M}^{(C2,E2\to M1)S=1}$ | : | $\hat{P}^{(11,2)1}$ | $\to$ | $\neq 0$ | $fm^5$ | P33 |
| $\mathcal{M}^{(C1\to E1)S=1}$ | : | $P^{(01,01)1}$ | $\to$ | $0$ | $fm^3$ | D13,S11 |
| $\mathcal{M}^{(C1\to E1)S=0}$ | : | $\boxed{P^{(01,01)0}}$ | $\to$ | $-\sqrt{\frac{2}{3}}\frac{4\pi}{e^2}(\alpha_E)$ | $fm^3$ | D13,S11 |
| $\mathcal{M}^{(M2\to E1)S=1}$ | : | $\boxed{P^{(01,12)1}}$ | $\to$ | $-\frac{\sqrt{2}}{3}\frac{4\pi}{e^2}(\gamma_3)$ | $fm^4$ | D13 |
| $\mathcal{M}^{(C1,E1\to E1)S=1}$ | : | $\hat{P}^{(01,1)1}$ | $\to$ | $\neq 0$ | $fm^4$ | D13,S11 |
| $\mathcal{M}^{(C1,E1\to E1)S=0}$ | : | $\hat{P}^{(01,1)0}$ | $\to$ | $\neq 0$ | $fm^4$ | D13,S11 |

## 2.2 Results at MAMI

The absolute cross sections $d^5\sigma^{exp}$ have been measured at the 855 MeV Mainz Microtron MAMI [11]. The scattered electron was detected in coincidence with the recoiling proton in two high-resolution spectrometers. The photon production process was selected by a cut on the missing mass around zero.

The aim of this first VCS experiment below pion threshold was to measure the five-fold differential cross sections in a wide photon angular range, at 5 values of the photon momentum q′: 33.6, 45, 67.5, 90, and 111.5 MeV/c (presentation in Fig. 2). The 3 other kinematical variables were held fixed, namely the virtual photon momentum, q = 600 MeV/c ($\tilde{Q}^2$ = 0.33 GeV$^2$), the virtual photon polarization $\epsilon$ = 0.62, the out-of-plane angle $\varphi$ around 0° and 180° (as the two spectrometers are moving in the same plane). The spherical angles $\theta$ and $\varphi$ are defined such that $\varphi$ = 0° corresponds to the half plane containing the electron momenta. To ease the presentation the data are plotted with $\theta$ ranging from -180° to +180°; the negative values corresponding in fact to $\varphi$ = 180°. The wide range of $\theta$ from -141° to +6° covers the backward direction relative to the incoming and outgoing electrons. Here, the VCS contributions are dominant because the electron radiations (BH) are emitted predominantly in the electron directions.

The cross sections $d^5\sigma^{BH+Born}$ are presented by the solid lines. At small photon momentum q′ = 33.6 MeV/c the agreement between the radiatively corrected data and $d^5\sigma^{BH+Born}$ is excellent, and the deviation from this known cross section increases when q′ increases, as expected from the effect of the proton polarizabilities.

Fig. 3 shows the behaviour of $(d^5\sigma - d^5\sigma^{BH+Born})/\phi$q′ as a function of the real photon momentum q′ for the 14 measured scattering angles $\theta$. As is apparent in this figure, there is no strong evolution with the real photon momentum. Therefore we make the hypothesis that there is no q′ dependence in $(d^5\sigma - d^5\sigma^{BH+Born})/\phi$q′. $\psi_0$ is then determined at each

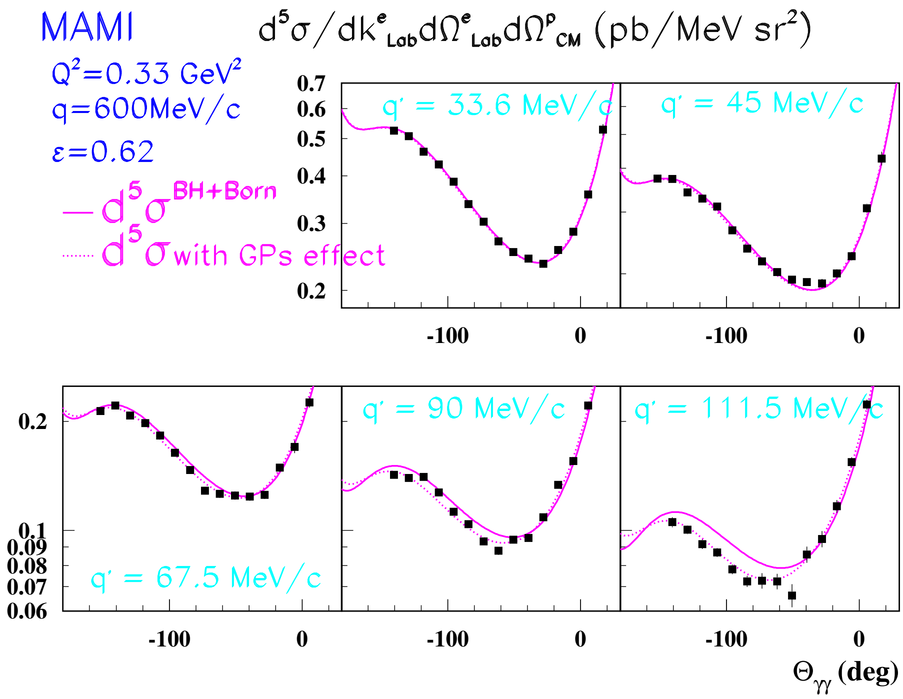


Figure 2: *Differential cross sections for the reaction* $ep \to ep\gamma$ *as a function of* $\theta$ *for fixed* $\mathrm{q}, \epsilon, \varphi$ *and for five values of the real photon momentum* $\mathrm{q}'$. *The known part of the cross section* $d^5\sigma^{BH+Born}$, *is presented by the solid lines. The experimental data points* $d^5\sigma^{exp}$ *deviate from the solid lines as* $\mathrm{q}'$ *increases - the effect of the proton polarizabilities. The dotted lines represent the expected cross sections with the effect of the polarizabilities measured by the two structure functions deduced from this experiment.*

scattering angle $\theta$ by the mean value of the data at the 5 photon energies. Fig. 4 presents the complete data set (for the 14 angles) of $\psi_0/v2$ as a function of $v1/v2$ (cf. Eq. (2)). The data are reasonably well aligned, which suggests that the higher order terms in the expansion of the cross section (cf. Eq. (1)) are unimportant. This good alignment for a wide angular range is also indicative of the consistency of the experimental data. We extract the two structure functions $P_{LL} - P_{TT}/\epsilon$ and $P_{LT}$ as the slope and intercept of a linear fit to the data (according Eq. (2)).

Two structure functions $\mathbf{P_{LL}} - \mathbf{P_{TT}}/\epsilon$ and $\mathbf{P_{LT}}$ are determined from the measured cross sections. These structure functions are the sum of two contributions (cf. Eq. 3) : one scalar related to the electric $\alpha_E$ and magnetic $\beta_M$ polarizabilities measured in RCS and one spin-dependent. The last contribution vanishes at $Q^2 = 0$. Fig. 5 shows the two VCS MAMI results with their systematic errors compared with the RCS results and two predictions : an isobaric model based on an effective Lagrangian (ELM) [7] and the chiral perturbation theory (ChPT) [5]. The VCS MAMI result seems to indicate a large spin-dependent contribution, which is not at all reproduced by the ELM. The limitation of models based on phenomenological lagrangian or constituent quarks which describes with success the nucleon resonances is that they have no relationship to chiral symmetry, an important property of QCD. The success of ChPT seems to be due to this most general and consistent approach, which emphasizes the important role of the pion cloud. Its role seems to be determining in $P^{(11,00)1}$ comparatively to the quarks. This GP can be

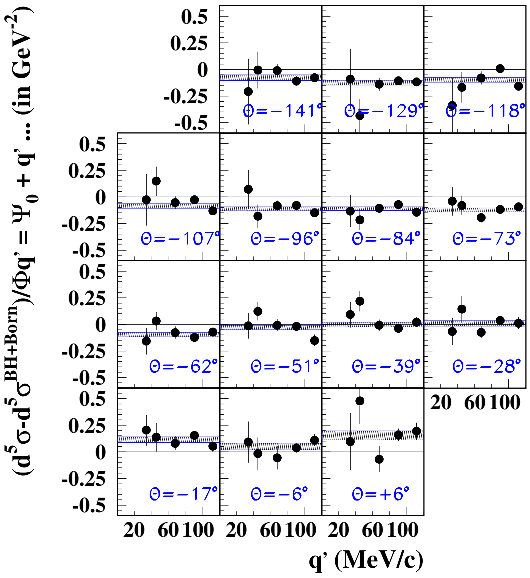

Figure 3: $(d^5\sigma - d^5\sigma^{BH+Born})/\phi q'$ *studied as a function of the real photon momentum* q′ *for the 14 measured scattering angles* $\theta$. *The intercept at origin is* $\psi_0$. *In a first method it is determined at each scattering angle* $\theta$ *by the mean value in the investigated real photon momentum range (dashed area) as no strong evolution with* q′ *is revealed experimentally.*

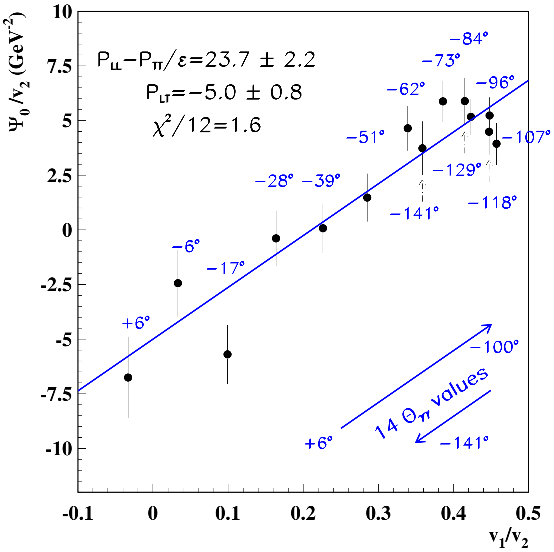

Figure 4: *Compilation of the complete data set (for the 14 angles) of* $\psi_0/v2$ *as a function of* $v1/v2$. *The data are reasonably well aligned; the errors indicated are statistical only. This allows to extract the two structure functions* $P_{LL} - P_{TT}/\epsilon$ *and* $P_{LT}$ *by linear regression (according Eq. (2)), with statistical errors and the* $\chi^2$ *given.*

interpreted by a Coulomb scattering applied on a nucleon placed in a magnetic field. This latter flips the spin of the quarks which hardly modifies the charge density, and only the pion cloud is seen by the Coulomb scattering. The complete description of the evolution of the two structure functions with $Q^2$ will be provided by the VCS experiments performed both at JLAB ($Q^2$ =1 and 1.9 GeV$^2$) and MIT-Bates ($Q^2$ = 0.05 GeV$^2$). To go beyond, that is to measure independently all the scalar and spin-dependent polarizabilities, it is necessary to perform a double polarization experiment.

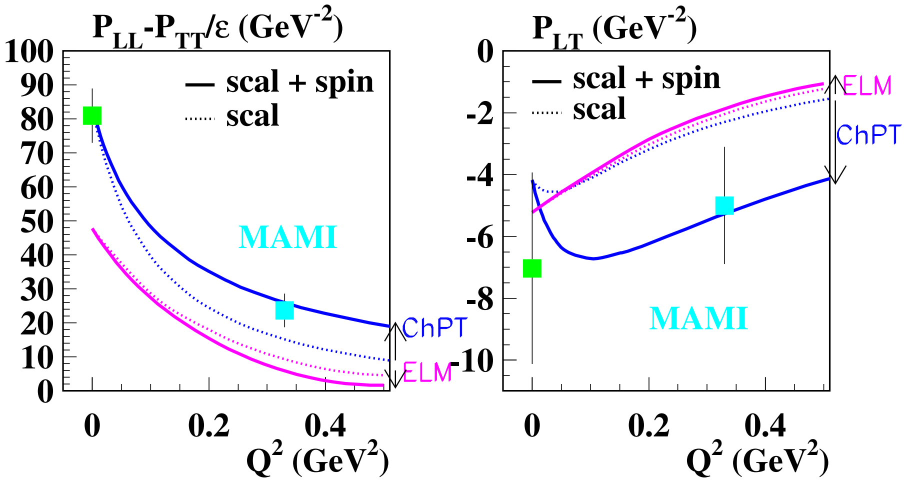


Figure 5: *Presentation of the two structure functions* $\mathbf{P_{LL}} - \mathbf{P_{TT}}/\epsilon$ *and* $\mathbf{P_{LT}}$ *as a function of* $Q^2$*. The RCS and VCS MAMI results are reported. 2 theoretical predictions are shown : Effective Lagrangian model and Chiral Perturbation Theory*

# 3 Other possible VCS experiments

Before the investigation of double polarization experiments, we can consider other possibilities with unpolarized experiment.

- investigation in $Q^2$ at MAMI:
  The value of $Q^2 = 0.33$ GeV$^2$ at MAMI has been chosen in such a way that the proton phase space is optimized for the proton spectrometer acceptance. The larger the value of $Q^2$, the smaller is the proton phase space due to the Lorentz boost. The maximum value is given by the maximum momentum reached in the spectrometer. An investigation of an in-plane experiment can be envisaged downto $Q^2 = 0.15$ GeV$^2$ (to keep the proton momentum sufficiently high to escape the target) and would complete Fig. 5.

- investigation in $\epsilon$ at MAMI or transverse-longitudinal separation:
  The advantage of an experiment at the same $Q^2$, but with an other value of $\epsilon$ is to provide a separation of one structure function $\mathbf{P_{LL}} - \mathbf{P_{TT}}/\epsilon$ in the two components $\mathbf{P_{LL}}$ and $\mathbf{P_{TT}}$. The first one is only related to the polarizability $P^{(0101)0}$ which has as limit at $Q^2 = 0$ the well known electric $\alpha_E$ polarizability. With the higher energy of the electron beam available at MAMI-C after 2004, we can envisage to do a measurement at higher $\epsilon$. If the maximum outgoing electron momentum is fixed by the limit of the spectrometer, we can reach $\epsilon$=0.80 which is unfortunately not so far from the actual value $\epsilon$=0.62 in order to provide a sufficient lever arm for an $\epsilon$ separation. We consider to submit a further proposal on this purpose in the future.

- investigation above the pion threshold:
  The dispersive formalism provides a new tool to analyze VCS experiments above the

pion threshold, thus increasing the sensitivity to the generalized polarizabilities [14]. We are also considering this possibility for a further experiment.

# 4 Double Polarized VCS experiment

## 4.1 Theoretical Framework

A double polarization VCS experiment with the polarized electron beam available at MAMI and a measurement of the recoil polarization of the outgoing proton in a focal plane polarimeter can be considered. The theoretical framework of such experiment has been developed by Vanderhaeghen and Guichon [3, 15]. Below pion production threshold, the VCS amplitude is purely real, and all single polarization observables are zero. So only double polarization experiment observables can disentangle the GPs. For a polarized electron of pure helicity state $h = \pm 1/2$ (longitudinal polarization $\xi_e = 2hk/m_e$), we can measure the average polarization $\vec{\mathcal{P}}$ of the recoil proton along the 3 vectors $(\vec{e}_{x_{cm}}, \vec{e}_{y_{cm}}, \vec{e}_{z_{cm}})$ associated to the virtual photon direction in the photon-proton CM as defined in Fig 6.

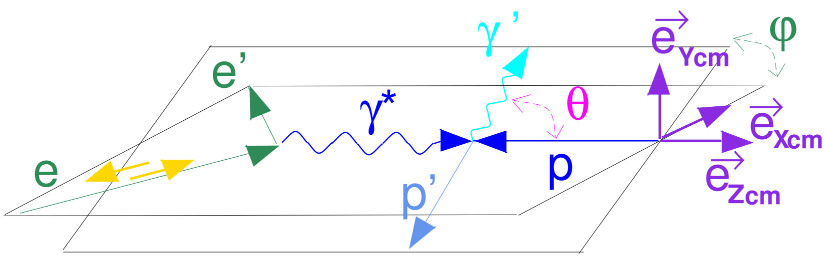


Figure 6: *Kinematics for the $p(\vec{e}, e'\vec{p'})\gamma$ reaction*

We can define for the 3 axes:

$$\vec{\mathcal{P}} \cdot \vec{e}(i) = \frac{d^5\sigma\left[\xi_e = \frac{2hk}{m_e}, \vec{\xi_p} = \vec{e}(i)\right] - d^5\sigma\left[\xi_e = \frac{2hk}{m_e}, \vec{\xi_p} = -\vec{e}(i)\right]}{d^5\sigma\left[\xi_e = \frac{2hk}{m_e}, \vec{\xi_p} = \vec{e}(i)\right] + d^5\sigma\left[\xi_e = \frac{2\ hk}{m_e}, \vec{\xi_p} = -\vec{e}(i)\right]} = \frac{\Delta d^5\sigma(h,i)}{2 \cdot d^5\sigma} \tag{4}$$

We obtain a similar low energy predictions as in Eq. 1:

$$\Delta d^5\sigma(h,i) = \Delta d^5\sigma^{BH+Born}(h,i) + \phi \mathrm{q}' \Delta\Psi_0(h,i) + \phi\mathcal{O}(\mathrm{q}'^2) \tag{5}$$

Finally we are left with 4 observables :

$$\begin{aligned}
\Psi_0 &= v_1(\theta,\varphi)(\mathbf{P_{LL}} - \mathbf{P_{TT}}/\epsilon) + v_2(\theta,\varphi)\mathbf{P_{LT}} \\
\Delta\Psi_0(h,z) &= (4h)\ \ [v_1^z(\theta,\varphi)\mathbf{P_{TT}} + v_2^z(\theta,\varphi)\mathbf{P^z_{LT}} + v_3^z(\theta,\varphi)\mathbf{P'^z_{LT}}] \\
\Delta\Psi_0(h,x) &= (4h)\ \ [v_1^x(\theta,\varphi)\mathbf{P^\perp_{LT}} + v_2^x(\theta,\varphi)\mathbf{P^\perp_{TT}} + v_3^x(\theta,\varphi)\mathbf{P'^\perp_{TT}} + v_4^x(\theta,\varphi)\mathbf{P'^\perp_{LT}}] \\
\Delta\Psi_0(h,y) &= (4h)\ \ [v_1^y(\theta,\varphi)\mathbf{P^\perp_{LT}} + v_2^y(\theta,\varphi)\mathbf{P^\perp_{TT}} + v_3^y(\theta,\varphi)\mathbf{P'^\perp_{TT}} + v_4^y(\theta,\varphi)\mathbf{P'^\perp_{LT}}]
\end{aligned} \tag{6}$$

Only 6 structure functions are independent: $\mathbf{P_{LL}}, \mathbf{P_{TT}}, \mathbf{P_{LT}}, \mathbf{P^{z}_{LT}}, \mathbf{P'^{z}_{LT}}$ and $\mathbf{P'^{\perp}_{LT}}$. ($\mathbf{P^{\perp}_{LT}}$ is a combination of $\mathbf{P_{TT}}$ and $\mathbf{P_{LL}}$, $\mathbf{P^{\perp}_{TT}}$ a combination of $\mathbf{P^{z}_{LT}}$ and $\mathbf{P_{LT}}$, $\mathbf{P'^{\perp}_{TT}}$ a combination of $\mathbf{P'^{z}_{LT}}$ and $\mathbf{P_{LT}}$).

$$
\begin{aligned}
\mathbf{P_{LL}} &= aP^{(01,01)0} \\
\mathbf{P_{TT}} &= \qquad\qquad c_1 P^{(11,11)1} + c_2 P^{(01,12)1} \\
\mathbf{P_{LT}} &= bP^{(11,11)0} \qquad\qquad + c_3[P^{(11,00)1} + d_1 P^{(11,02)1}] \\
\mathbf{P^{z}_{LT}} &= \qquad\qquad c_4 P^{(11,11)1} + c_3[P^{(11,00)1} + d_1 P^{(11,02)1}] \\
\mathbf{P'^{z}_{LT}} &= \qquad\qquad c_5 P^{(11,11)1} + c_6[P^{(11,00)1} + d_1 P^{(11,02)1}] \\
\mathbf{P'^{\perp}_{LT}} &= \qquad\qquad [d_2 P^{(11,00)1} + d_3 P^{(11,02)1}]
\end{aligned}
\tag{7}
$$

The $v_i^j(\theta, \varphi)$ in Eq. 6 are kinematical factors. If the out-of-plane angle $\varphi$ remains close to $0°$ or $180°$, with very rough approximations we can give the evolutions of these factors with $\theta$ and $\varphi$ :

$$
\begin{aligned}
v_1 = v_1^z \sim v_1^x &\propto sin\theta \\
v_2 \sim v_2^z \sim v_2^x &\sim constant \\
v_3^z \sim v_3^x &\propto cos\theta \\
v_4^x &\propto sin\varphi \sim 0 \\
\forall i, v_i^y &\propto sin\varphi \sim 0
\end{aligned}
\tag{8}
$$

With an in-plane double polarization experiment we can get 5 independent structure functions : $\mathbf{P_{LL}}, \mathbf{P_{TT}}, \mathbf{P_{LT}}, \mathbf{P^{z}_{LT}}, \mathbf{P'^{z}_{LT}}$. $\mathbf{P'^{\perp}_{LT}}$ is only reached in an out-of-plane experiment and will disentangle completely the 6 GPs.

## 4.2 Definition of a future experiment at MAMI

Double polarization asymmetries have been defined along the 3 vectors $(\vec{e}_{x_{cm}}, \vec{e}_{y_{cm}}, \vec{e}_{z_{cm}})$ associated to the virtual photon in the photon-proton CM. A rotation of characteristic angles $(\theta, \varphi)$ followed by a Wigner rotation to go from CM to lab frame is necessary to define the double polarization asymmetries along the 3 vectors $(\vec{e}_{x_{lab}}, \vec{e}_{y_{lab}}, \vec{e}_{z_{lab}})$ where $\vec{e}_{z_{lab}}$ is the direction of the outgoing proton in the lab. Double polarization asymmetries will be measured after the spin precession in the spectrometer along 3 vectors $(\vec{e}_{x_{fp}}, \vec{e}_{y_{fp}}, \vec{e}_{z_{fp}})$ associated with the direction of the outgoing proton detected in the polarimeter positioned in the focal plane.

We are investigating the possibility to realize an out-of-plane measurement by using the ability of the electron spectrometer to move out-of-plane, in order to measure the three components using the complete acceptance of the spectrometers. Nevertheless at the time of this presentation, we have made the “simple” hypothesis of an in-plane measurement. The goal is then to extract 5 GPs : $P^{(01,01)0}$, $P^{(11,11)0}$, $P^{(11,11)1}$, $P^{(01,12)1}$ and a combination of $P^{(11,00)1}$ and $P^{(11,02)1}$ Moreover for the following predictions, the spin precession is considered at the first order, only for a central trajectory. The geometry is depicted in Fig 7, and we can summarize the different polarization asymmetries along the three frames by the following scheme:

$$\begin{array}{lll}
\mathcal{P}_z^{cm} & \mathcal{P}_z^{lab} = \mathcal{R}(\mathcal{P}_z^{cm}, \mathcal{P}_x^{cm}) & \mathcal{P}_z^{fp} \text{ not measured} \\
\mathcal{P}_x^{cm} & \mathcal{P}_x^{lab} = \mathcal{R}(\mathcal{P}_z^{cm}, \mathcal{P}_x^{cm}) & \mathcal{P}_x^{fp} = \mathcal{P}_x^{lab} \\
\mathcal{P}_y^{cm} \sim 0 & \mathcal{P}_y^{lab} \sim 0 & \mathcal{P}_y^{fp} = sin\chi \mathcal{P}_z^{lab} + cos\chi \mathcal{P}_y^{lab}
\end{array}$$

$$\nwarrow \text{ rotations } \nearrow \qquad \nwarrow \text{ spin precession } \nearrow$$

where we consider only in-plane experiment ($sin\varphi \sim 0$), and a precession of the spin-vector in a pure dipole (rotation of an angle $\chi = \gamma_p \cdot 1.79 \cdot \delta$ with a magnetic spectrometer angular deviation $\delta$ and a proton Lorentz factor $\gamma_p$).

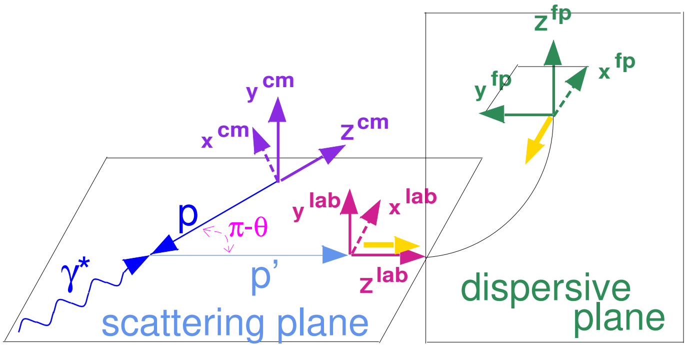


Figure 7: *definition of the different frames* $(\vec{e}_{x_{cm}}, \vec{e}_{y_{cm}}, \vec{e}_{z_{cm}})$, $(\vec{e}_{x_{lab}}, \vec{e}_{y_{lab}}, \vec{e}_{z_{lab}})$, $(\vec{e}_{x_{fp}}, \vec{e}_{y_{fp}}, \vec{e}_{z_{fpm}})$.

The focal plane proton-polarimeter is described in the reference [16] and is fully operational. It consists of a carbon analyser of variable thickness and two double-planes of horizontal drift chambers. We can summarize its qualities by an average efficiency of 2.5% in the proton momentum range 472-736 MeV/c (which will be used for the proposed experiment) and an analysing power varying around 0.5.

Theoretical predictions presented in Fig. 8, have been made by computing the BH and Born contributions (dotted lines) and the effect of the GPs in the Heavy Baryon Chiral Pertubation GPs (solid lines). We can see the VCS double polarization asymmetry obtained along the relevant directions $\vec{e}_{x_{cm}}$, $\vec{e}_{z_{cm}}$, $\vec{e}_{x_{fp}}$ and $\vec{e}_{y_{fp}}$. We can note that the polarization asymmetries are rather flat along the CM axes, while they vary rapidly with the angle $\theta$ along the focal plane axes. The good reproduction of the BH+Born prediction at low real photon momentum q$'$ (where no effect of GPs is expected) will insure a good control of the $\theta$ resolution and will give confidence to the determination of an asymmetry deviation at larger q$'$. The asymmetry deviation is predicted smaller than 10% and is represented by the dash-dotted line (scaled by a factor 10).

The asymmetry deviation along the same axes is studied with its different ingredients in Fig. 9. The effect of the polarizability $P^{(0101)0}$ (related to the electric $\alpha_E$ polarizability at $Q^2 = 0$) and the one of the polarizability $P^{(1111)0}$ (related to the magnetic $\beta_M$ polarizability at $Q^2 = 0$) are indicated respectively in dash-dotted line and dashed line. The resulting effect of the non spin dependent polarizabilities is designed by the solid blue line. The addition of the spin dependent polarizabilities is presented by the solid purple line. There exists no trivial singular point in $\theta$ where the effect of the spin dependent polarizabilities is clearly maximized. So the strategy will be to measure the complete angular range in $\theta$ and to extract the 5 GPs from the angular evolution as it was done in the previous experiment (see Fig 4).

The angular evolutions of the three relevant quantities obtained in this in-plane measurement, $\Psi_0$, $\Delta\Psi_0(h,z)$ and $\Delta\Psi_0(h,x)$, are represented in the Figure 10. With a luminosity of $3.10^{37}$ cm$^{-2}$s$^{-}1$, a beam polarization around 80% and a focal plane polarimeter efficiency of the MAMI spectrometer of about 2.5% (in the range 472-736 MeV/c), a very precise measurement of the double polarisation asymmetry (with errors of 2% in Fig 8) will require about 2000 hours of data taking and will give the error bars presented in Fig 10. It has to be emphasized that a wide angular range measurement will insure the coherence of the results as it was a crucial point in the first unpolarized experiment. This future experiment which should solve the determination of the GPs, cannot be achieved without a good strategy and a very delicate expertise of the complete apparatus.

It is the reason why we have a request of **300 hours** to do some tests in the coming year. The principal aim is to measure the double polarization asymmetry at a low value of the real photon momentum $q'$=33.6 MeV/c with very good statistics. The goal is to reproduce the BH+Born polarization asymmetry in order to study the systematic uncertainties. Two questions will be investigated:

- the complete study of the spin precession at a very high level of precision and the influence of the large acceptance of the spectrometers,

- the resolution in $\theta$ which is a principal key of the determination of the GPs as they are extracted from the angular evolution of the asymmetry deviation from the BH+Born contribution.

In parallel an extensive work on the simulation of the complete set-up is being performed. A more complete proposal for this measurement which implies great statistic and systematic precisions can then be formulated and will take benefit of this first run.

# References


[1] P.A.M. Guichon, G.Q. Liu and A.W. Thomas, Nucl. Phys. **A591**, 606 (1995).

[2] D. Drechsel *et al.*, Phys. Rev. **C55**, 424 (1997); Phys. Rev. **C57**, 941 (1998).

[3] P.A.M. Guichon and M. Vanderhaeghen, Progress in Particle and Nuclear Physics **Vol. 41**, 125 (1998).

[4] B.E. MacGibbon *et al.*, Phys. Rev. **C52**, 2097 (1995).

[5] T.R. Hemmert, B.R. Holstein, G. Knöchlein and S. Scherer, Phys. Rev. **D55**, 2630 (1997); Phys. Rev. Lett. **79**, 22 (1997).

[6] A. Metz and D. Drechsel, Z. Phys. **A356**, 351 (1996); Z. Phys. **A359**, 165 (1997).

[7] M. Vanderhaeghen, Phys. Lett. **B368**, 13 1996.

[8] G.Q.Liu, A.W.Thomas and P.Guichon, Aust. J. Phys. **49**, 905 (1996).

[9] B. Pasquini, S. Scherer and D. Drechsel, MKPH-T-00-17, ECT*-00-009, (August 2000).

[10] F.E. Low, Phys. Rev. **96**, 1428 (1954); Phys. Rev. **110**, 974 (1958).

[11] J. Roche *et al.*, Phys. Rev. Lett. **85**, 708 (2000).

[12] P.Y. Bertin, P.A.M. Guichon and Ch. Hyde-Wright, spokespersons TJNAF proposal, E-93-050, (1993).

[13] J. Shaw and R. Miskimen, spokespersons MIT-Bates Proposal, (1997).

[14] B. Pasquini, D. Drechsel, M. Gorchtein, A. Metz and M. Vanderhaeghen, Phys. Rev. **C62**, 052201 (2000).

[15] M. Vanderhaeghen, Phys. Lett. B **402** 243 (1997).

[16] Th. Pospischil *et al.*, submitted to Nucl. Instr. and Meth., (see http://wwwa1.kph.uni-mainz.de/A1/publications/).

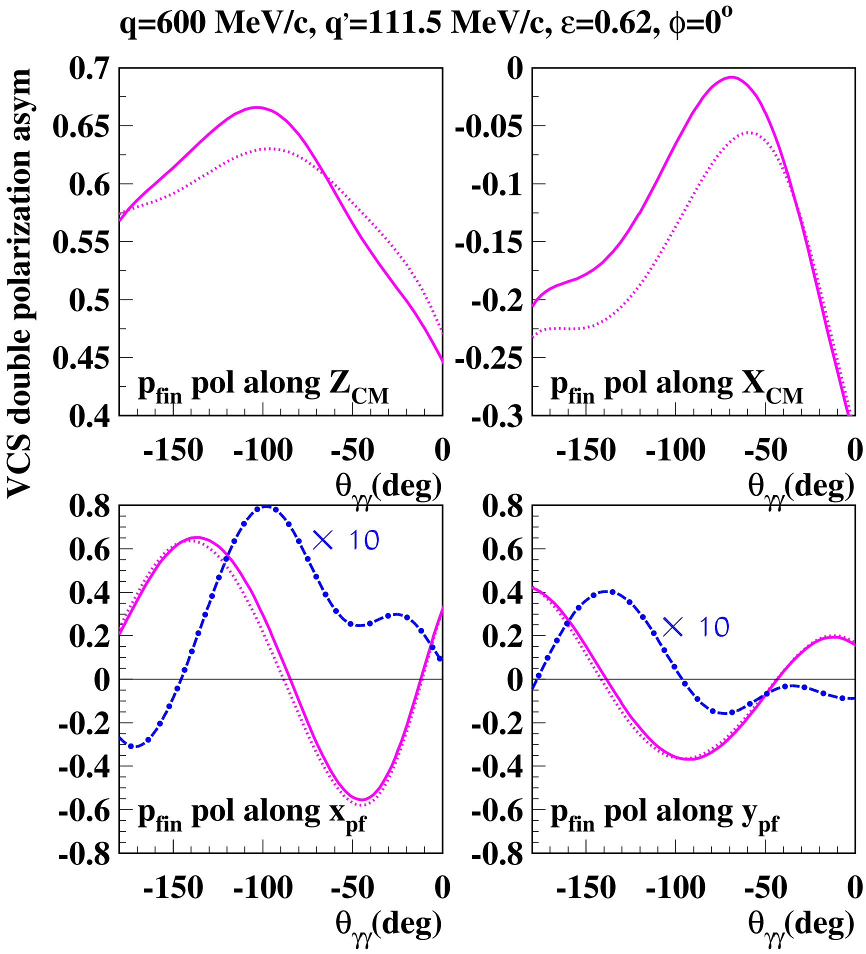


Figure 8: *Predictions for a double polarization experiment at MAMI. Double polarization asymmetries are determined along* $z_{cm}$ *and* $x_{cm}$ *in the upper part, and along* $x_{fp}$ *and* $y_{fp}$ *where they will be measured. The dotted lines indicate the BH+Born contribution only, the GPs effects are included in the solid lines. The difference (multiplied by 10) is indicated in dash-dotted line.*

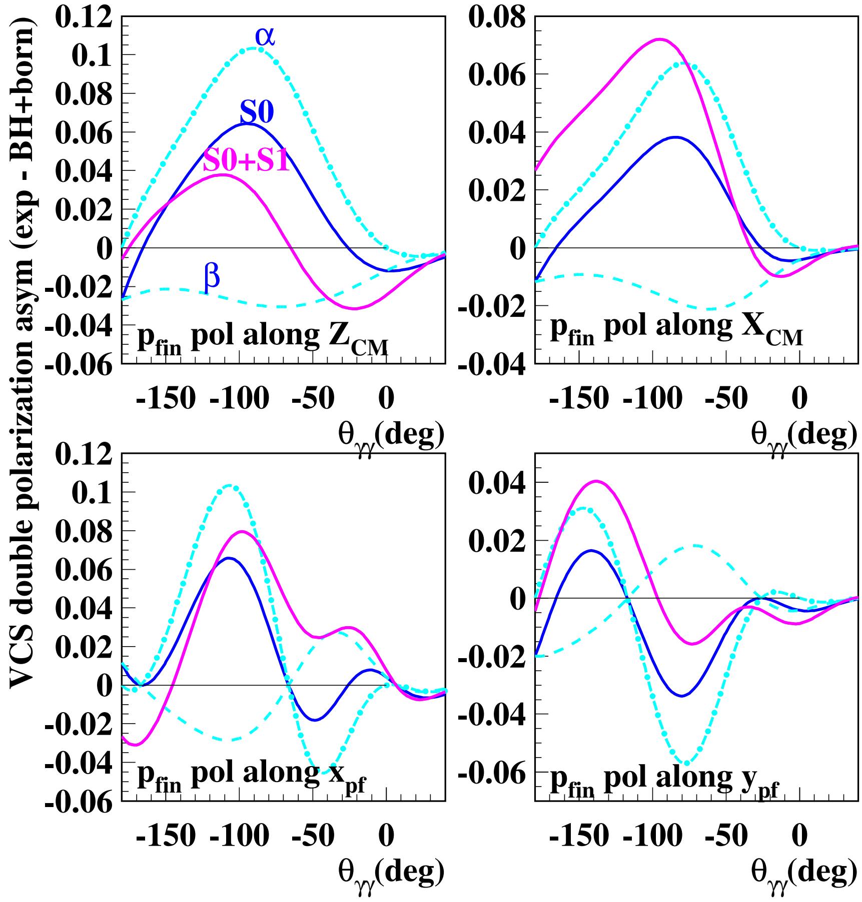


Figure 9: *Deviation of the double polarization VCS asymmetry from the BH+Born contribution. The effects of the polarizabilities $P^{(0101)0}$ (related to the electric $\alpha_E$ polarizability at $Q^2 = 0$) and $P^{(1111)0}$ (related to the magnetic $\beta_M$ polarizability at $Q^2 = 0$) are indicated respectively in dash-dotted line and dashed line. The resulting effect of the non spin dependent polarizabilities is designed by the solid blue line (S0). The addition of the spin dependent polarizabilities is presented by the solid purple line (S0+S1). There exists no trivial singular point in $\theta$ where the effect of the spin dependent polarizabilities is clearly maximized.*

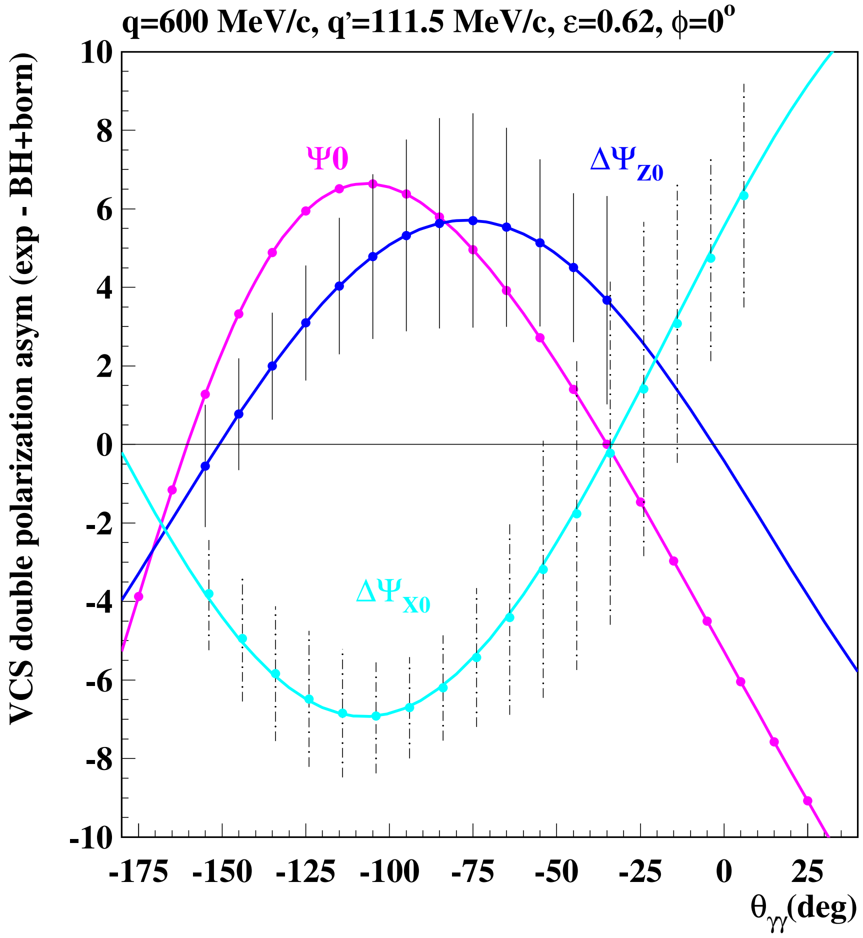


Figure 10: *Angular evolutions of the three relevant quantities obtained in an in-plane measurement,* $\Psi_0$*,* $\Delta\Psi_0(h,z)$ *and* $\Delta\Psi_0(h,x)$ *described in equation (6). The investigated angular range with the accuracy obtained in 2000 hours at* $\mathrm{q}' = 111.5$ *MeV/c would allow to extract the individual GPs.*